J|A|C|S
ARTICLES
Published on Web 01/26/2002

Stereochemistry of Lactide Polymerization with Chiral Catalysts: New Opportunities for Stereocontrol Using Polymer Exchange Mechanisms

Tina M. Ovitt and Geoffrey W. Coates*

Contribution from Baker Laboratory, Department of Chemistry and Chemical Biology, Cornell University, Ithaca, New York 14853-1301

Received August 27, 2001

Abstract: The synthesis of chiral aluminum and yttrium alkoxides and their application for lactide polymerization are reported. The complexes (SalBinap)MOR [**4**, M = Al, R = ^{i}Pr; **5**, M = Y, R = $(CH_2)_2$-NMe_2] are synthesized by reacting the ligand (SalBinap)H_2 [2,2′-[(1,1′-binaphthalene)-2,2′-diylbis(nitrilomethylidyne)]bisphenol] with the appropriate metal trisalkoxide. While enantiomerically pure yttrium complex **5** did not effect stereocontrol in the polymerization of either *meso*- or *rac*-lactide, homochiral **4** was found to exhibit excellent stereocontrol in a range of lactide polymerizations. Enantiomerically pure **4** polymerizes *meso*-lactide to syndiotactic poly(lactic acid) (PLA), while *rac*-**4** polymerizes *meso*- and *rac*-lactide to heterotactic and isotactic stereoblock PLA, respectively. On the basis of the absolute stereochemistry of ring-opening of *meso*-lactide using (*R*)-**4**, a polymer exchange mechanism is proposed to account for the PLA microstructures resulting from *rac*-**4**.

Introduction

Stereochemistry is one of the main factors that determine the physical and mechanical properties of a polymeric material, as well as its rate of chemical and biological degradation. Polymers that have stereocenters in the repeat unit can exhibit two structures of maximum order, isotactic and syndiotactic.[1] Isotactic polymers contain sequential stereocenters of the same relative configuration, while syndiotactic polymers contain sequential stereocenters of opposite relative configuration. These stereoregular polymers are typically crystalline and have found use in many applications. Homogeneous single-site catalysts have proven to be one of the most promising methodologies for the synthesis of stereoregular polymers.[2] With single-site catalysts, enchainment of a monomer occurs at a metal center (M, the active site) that is bound by an organic ligand (L). This ancillary ligand remains bound throughout the catalytic reaction, modulating the reactivity of the metal center. Typical single-site catalysts for lactone polymerization are of the form L_nMOR, where the alkoxide group (OR) is capable of propagation. These complexes are conceptually different from typical lactone polymerization catalysts of the form $M(OR)_n$, which do not possess a permanent ancillary ligand. In contrast to conventional heterogeneous catalysts, homogeneous catalysts have been designed that can control polymer molecular weights, molecular weight distributions (MWDs), comonomer incorporation, and stereochemistry. Despite significant progress toward the development of well-defined catalysts for olefin polymerization, relatively few single-site catalysts have been reported for the ring-opening polymerization of heterocycles such as epoxides and lactones.[3−27]

(1) Farina, M. *Top. Stereochem.* **1987**, *17*, 1−111.
(2) Coates, G. W. *Chem. Rev.* **2000**, *100*, 1223−1252.
(3) For reviews on lactone polymerization, see: (a) O'Keefe, B. J.; Hillmyer, M. A.; Tolman, W. B. *J. Chem. Soc., Dalton Trans.* **2001**, 2215−2224. (b) Duda, A.; Penczek, S. *Polymers from Renewable Resources: Biopolyesters and Biocatalysis*; ACS Symposium Series 764; American Chemical Society: Washington, DC, 2000; pp 160−198. (c) Kuran, W. *Prog. Polym. Sci.* **1998**, *23*, 919−992. (d) Loefgren, A.; Albertsson, A.; Dubois, P.; Jerome, R. *J. Macromol. Sci., Rev. Macromol. Chem. Phys.* **1995**, *C35*, 379−418.
(4) For some recent, leading references concerning single-site catalysts for lactone polymerization, see refs 5−27.
(5) Aida, T.; Inoue, S. *Acc. Chem. Res.* **1996**, *29*, 39−48.
(6) Inoue, S. *J. Polym. Sci., Part A: Polym. Chem.* **2000**, *38*, 2861−2871.
(7) Spassky, N.; Dumas, P.; Le Borgne, A.; Momtaz, A.; Sepulchre, M. *Bull. Soc. Chim. Fr.* **1994**, *131*, 504−514.
(8) Spassky, N.; Wisniewski, M.; Pluta, C.; Le Borgne, A. *Macromol. Chem. Phys.* **1996**, *197*, 2627−2637.
(9) Chisholm, M. H.; Eilerts, N. W. *Chem. Commun.* **1996**, 853−854.
(10) Chisholm, M. H.; Eilerts, N. W.; Huffman, J. C.; Iyer, S. S.; Pacold, M.; Phomphrai, K. *J. Am. Chem. Soc.* **2000**, *122*, 11845−11854.
(11) Cheng, M.; Attygalle, A. B.; Lobkovsky, E. B.; Coates, G. W. *J. Am. Chem. Soc.* **1999**, *121*, 11583−11584.
(12) Ovitt, T. M.; Coates, G. W. *J. Am. Chem. Soc.* **1999**, *121*, 4072−4073.
(13) Ovitt, T. M.; Coates, G. W. *J. Polym. Sci., Part A: Polym. Chem.* **2000**, *38*, 4686−4692.
(14) Chamberlain, B. M.; Cheng, M.; Moore, D. R.; Ovitt, T. M.; Lobkovsky, E. B.; Coates, G. W. *J. Am. Chem. Soc.* **2001**, *123*, 3229−3238.
(15) Yasuda, H.; Ihara, E. *Adv. Polym. Sci.* **1997**, *133*, 53−101.
(16) Okuda, J.; Kleinhenn, T.; Konig, P.; Taden, I.; Ngo, S.; Rushkin, I. L. *Macromol. Symp.* **1995**, *95*, 195−202.
(17) Beckerle, K.; Hultzsch, K. C.; Okuda, J. *Macromol. Chem. Phys.* **1999**, *200*, 1702−1707.
(18) Taden, I.; Kang, H. C.; Massa, W.; Spaniol, T. P.; Okuda, J. *Eur. J. Inorg. Chem.* **2000**, 441−445.
(19) Radano, C. P.; Baker, G. L.; Smith, M. R. *J. Am. Chem. Soc.* **2000**, *122*, 1552−1553.
(20) Chamberlain, B. M.; Sun, Y. P.; Hagadorn, J. R.; Hemmesch, E. W.; Young, V. G.; Pink, R.; Hillmyer, M. A.; Tolman, W. B. *Macromolecules* **1999**, *32*, 2400−2402.
(21) Chamberlain, B. M.; Jazdzewski, B. A.; Pink, R.; Hillmyer, M. A.; Tolman, W. B. *Macromolecules* **2000**, *33*, 3970−3977.
(22) Aubrecht, K. B.; Chang, K.; Hillmyer, M. A.; Tolman, W. B. *J. Polym. Sci., Part A: Polym. Chem.* **2001**, *39*, 284−293.
(23) Ko, B. T.; Lin, C. C. *Macromolecules* **1999**, *32*, 8296−8300.

10.1021/ja012052+ CCC: $22.00

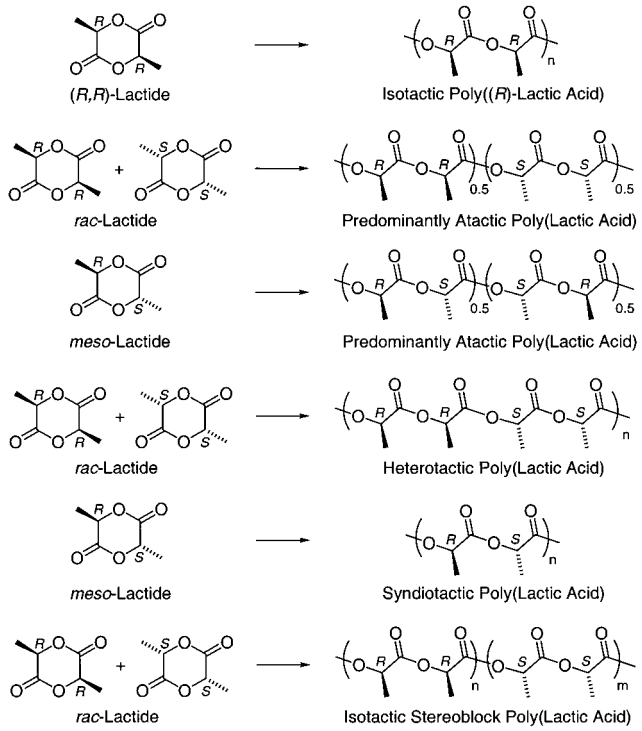

Figure 1. Poly(lactic acid) microstructures.

Poly(lactic acid)s (PLAs) are biocompatible and biodegradable materials with many potential medical, agricultural, and packaging applications.[28−31] PLAs are formed by the ring-opening of lactide (LA), a cyclic diester of lactic acid, by various metal alkoxide species (Figure 1). The ring-opening occurs through a coordination−insertion mechanism by cleavage of the acyl−oxygen bond with retention of configuration.[32−36] Prior to work in our laboratory, available microstructures were limited to atactic, partially heterotactic, and isotactic PLA. For example, amorphous atactic polymers are afforded from the polymerization of *rac*-lactide or *meso*-lactide with aluminum tris(alkoxide)[34,35] or tin bis(carboxylate)[36] catalysts. These atactic polymers possess random placements of -*RR*- and -*SS*- stereosequences for *rac*-lactide and -*RS*- and -*SR*- stereosequences for *meso*-lactide.

One of the most important advances in the control of PLA stereochemistry was reported by Spassky and co-workers,[8] who found the enantiomerically pure, chiral complex (*R*)-(SalBinap)-$AlOCH_3$ [(*R*)-**2**] (Scheme 1) exhibited high selectivity in the kinetic resolution of *rac*-lactide. At 70 °C, the catalyst exhibited a 20:1 preference for the polymerization of (*R*,*R*)-lactide over (*S*,*S*)-lactide (Figure 2). The polymerization proceeded by a living mechanism, as shown by the narrow MWD and control of the resultant polymer molecular weight by the monomer/catalyst ratio. At conversions less than 50%, the polymer microstructure was predominantly isotactic poly[(*R*)-lactic acid]. At conversions greater than 60%, only (*S*,*S*)-lactide remained. Due to the kinetic preference for the (*R*)-enantiomer, the reaction very slowly reached 100% conversion. The polymer formed presumably had a tapered stereoblock microstructure, where the monomer composition varied from all *R*-units to all *S*-units over the length of the polymer chain. The material exhibited a high melting temperature, T_m = 187 °C, relative to enantiopure isotactic material, which melts between 170 and 180 °C. This is strong evidence that a stereocomplex formed between the blocks of *R*-units and the blocks of *S*-units.

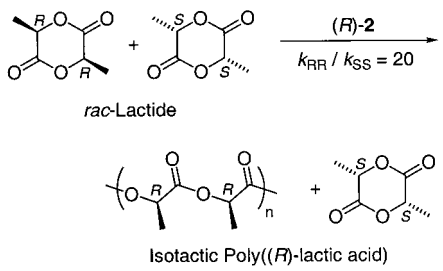

Figure 2. Kinetic resolution of *rac*-lactide.

We recently reported the synthesis of heterotactic PLA from *rac*-lactide with a single-site β-diiminate zinc alkoxide catalyst that controls stereochemistry by a chain-end control mechanism.[11,14,37] Kasperczyk et al.[38,39] have also synthesized heterotactic PLA from *rac*-lactide using lithium *tert*-butoxide aggregates. We have recently communicated the syntheses of syndiotactic[12] and stereoblock[13] PLAs through the use of single-site aluminum alkoxide catalysts. Chisholm has reported the synthesis of partially syndiotactic PLA using chiral tris(pyrazolyl) borate complexes.[10] Herein we expand upon these initial discoveries, and present a general approach for the synthesis of new polymer architectures using polymer exchange mechanisms.[40]

Results and Discussion

Complex Synthesis. In 1996, Spassky and co-workers reported the synthesis of (*R*)-**2** (Scheme 1), prepared by reaction of the chiral Schiff base (*R*)-(−)-(SalBinap)H_2 [(*R*)-**1**][41] with $AlEt_3$ in toluene at room temperature to yield (*R*)-(SalBinap)-AlEt.[8] Complex (*R*)-**2** was afforded by reaction of (*R*)-(SalBinap)AlEt with dry methanol. We repeated this preparation in our laboratory and found that the methanol mother liquor upon standing produces large colorless crystals of a bimetallic complex [(*R*)-**3**] which accounts for approximately 30% of the

(24) Cameron, P. A.; Jhurry, D.; Gibson, V. C.; White, A. J. P.; Williams, D. J.; Williams, S. *Macromol. Rapid Commun.* **1999**, *20*, 616−618.
(25) Dove, A. P.; Gibson, V. C.; Marshall, E. L.; White, A. J. P.; Williams, D. J. *Chem. Commun.* **2001**, 283−284.
(26) Giesbrecht, G. R.; Whitener, G. D.; Arnold, J. *J. Chem. Soc., Dalton Trans.* **2001**, 923−927.
(27) Huang, C. H.; Wang, F. C.; Ko, B. T.; Yu, T. L.; Lin, C. C. *Macromolecules* **2001**, *34*, 356−361.
(28) Chiellini, E.; Solaro, R. *Adv. Mater.* **1996**, *8*, 305−313.
(29) Swift, G. *Acc. Chem. Res.* **1993**, *26*, 105−110.
(30) Kricheldorf, H. R.; Kreiser-Saunders: I.; Juergens, C.; Wolter, D. *Macromol. Symp.* **1996**, *103*, 85−102.
(31) Ikada, Y.; Tsuji, H. *Macromol. Rapid Commun.* **2000**, *21*, 117−132.
(32) Kricheldorf, H. R.; Lee, S. R.; Bush, S. *Macromolecules* **1996**, *29*, 1375−1381.
(33) Stevels, W. M.; Dijkstra, P. J.; Feijen, J. *Trends Polym. Sci.* **1997**, *5*, 300−305.
(34) Dubois, P.; Jacobs, C.; Jérôme, R.; Tessié, P. *Macromolecules* **1991**, *24*, 2266−2270.
(35) Kowalski, A.; Duda, A.; Penczek, S. *Macromolecules* **1998**, *31*, 2114−2122.
(36) Kowalski, A.; Duda, A.; Penczek, S. *Macromolecules* **2000**, *33*, 689−695.
(37) Cheng, M.; Ovitt, T. M.; Hustad, P. D.; Coates, G. W. *Polym. Prepr. (Am. Chem. Soc., Div. Polym. Chem.)* **1999**, *40* (1), 542−543.
(38) Kasperczyk, J. E. *Macromolecules* **1995**, *28*, 3937−3939.
(39) Kasperczyk, J. E. *Polymer* **1999**, *40*, 5455−5458.
(40) For recent examples of stereoblock polymer synthesis using polymer exchange pathways, see: (a) Chien, J. C. W.; Iwamoto, Y.; Rausch, M. D.; Wedler, W.; Winter, H. H. *Macromolecules* **1997**, *30*, 3447−3458. (b) Chien, J. C. W.; Iwamoto, Y.; Rausch, M. D. *J. Polym. Sci., Part A: Polym. Chem.* **1999**, *37*, 2439−2445. (c) Lieber, S.; Brintzinger, H. H. *Macromolecules* **2000**, *33*, 9192−9199. (d) Boucard, V.; Moreau, M.; Dumas, P. *Macromol. Chem. Phys.* **2001**, *202*, 1974−1979.
(41) Bernardo, K. D.; Robert, A.; Dahan, F.; Meunier, B. *New J. Chem.* **1995**, *19*, 129−131.

Scheme 1

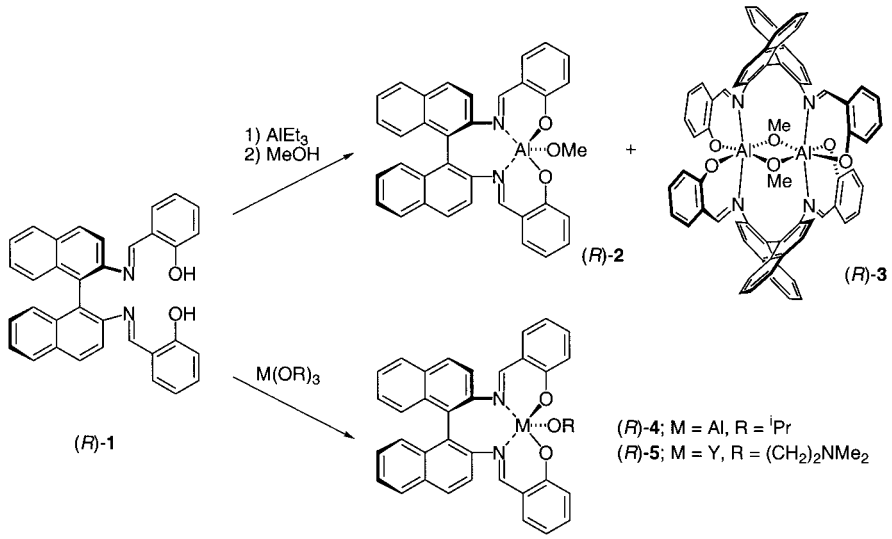

total reaction product (Scheme 1). A single crystal of this complex was studied by X-ray crystallography (Figure 3). The

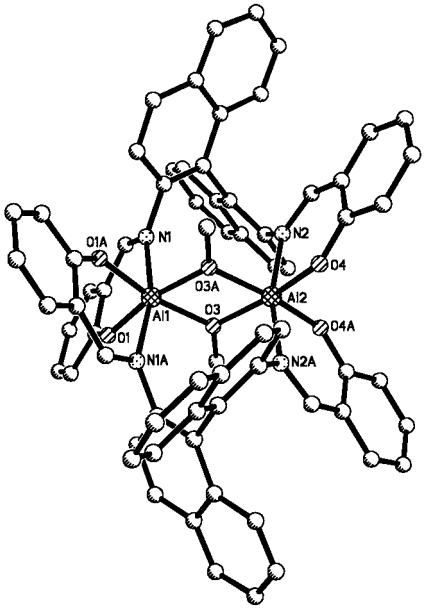

Figure 3. X-ray crystal structure of (*R*)-**3**.

SalBinap ligand of (*R*)-**3** spans two aluminum centers, and the cleft between the ligands is occupied by a methoxide group. The complex exhibits D_2 symmetry, and the core bond distances and angles are typical of those reported in the literature for aluminum salen complexes.[42] It is not currently clear whether (*R*)-**3** is formed by a redistribution of (*R*)-**2** after it is synthesized, or whether (μ-η^2-SalBinap)$_2$Al$_2$(μ-Et)$_2$ is the initial product that is methanolyzed to (*R*)-**3**. Although complex (*R*)-**3** was found to be a catalytically inactive byproduct of the synthesis of catalyst (*R*)-**2**, we decided to pursue a more efficient route to the synthesis of this class of compounds. We reasoned that a larger alkoxide group would favor the desired monometallic complexes because groups larger than an ethoxide are sterically larger than the cleft of **3**. Since an isopropoxide is a suitable mimic of the putative propagating secondary alkoxide bound to the metal, we decided to synthesize complex (*R*)-**4**.

The synthesis of (*R*)-(SalBinap)AlO^iPr [(*R*)-**4**] was achieved by adding freshly distilled Al(O^iPr)$_3$ to a toluene solution of (*R*)-**1**. After the mixture was stirred at 70 °C for 2 days, the solvent was removed in vacuo to yield (*R*)-**4** as a yellow solid. Despite repeated attempts, we were not able to obtain single crystals of (*R*)-**4**. The ^{1}H NMR spectrum of (*R*)-**4** suggests that the complex exhibits C_1 symmetry as exhibited by analogous yttrium compounds (vide infra).

We decided to also investigate yttrium-based complexes due to the established relations between group 3 and 13 metals, as well as the high activity of yttrium alkoxide complexes for lactone polymerization.[20,22,33,43] [(*R*)-(SalBinap)YO(CH$_2$)$_2$-NMe$_2$]$_2$ [(*R*)-**5**] was synthesized by adding Y(O(CH$_2$)$_2$NMe$_2$)$_3$ to a toluene solution of (*R*)-**1**. After the mixture was stirred at 70 °C for 1 day, the solvent was removed in vacuo to yield (*R*)-**5** as a crystalline yellow solid. A single crystal of this complex was subjected to X-ray structural analysis (Figure 4). (*R*)-**5** is an alkoxy-bridged dimer, with seven-coordinate yttrium centers ligated by (*R*)-**1** adopting a *cis*-β geometry and Δ chirality. We tentatively propose that the structure of (*R*)-**4**, for which no X-ray crystal structure could be obtained, is analogous to that of (*R*)-**5**.

Polymerization of *meso*-Lactide Using Enantiomerically Pure Catalysts. (*R*)-**5** was examined for the polymerization of *meso*-lactide (LA).[12] After 14 h at 70 °C, the reaction proceeded to 97% conversion ([LA] = 0.2 M in toluene, [LA]/[(*R*)-**5**] = 100). Analysis of the polymer microstructure using homonuclear decoupled ^{1}H NMR revealed that (*R*)-**5** forms atactic poly(lactic acid).

We then investigated (*R*)-**4** for the polymerization of *meso*-lactide ([LA] = 0.2 M in toluene, [LA]/[(*R*)-**4**] = 100) (Figure 5).[12] After 40 h at 70 °C, the reaction had proceeded to 94% conversion. Subsequently, the polymerization was performed at 70 °C for varying amounts of time (Table 1).[44] Gel permeation chromatography revealed M_n values (relative to polystyrene) close to the theoretical values and narrow MWDs (Table 1).

(42) Atwood, D. A.; Harvey, M. J. *Chem. Rev.* **2001**, *101*, 37−52.

(43) McLain, S. L.; Ford, T. M.; Drysdale, N. E. *Polym. Prepr. (Am. Chem. Soc., Div. Polym. Chem.)* **1992**, *33* (2), 463−464.

(44) A polymerization was performed at 50 °C for 40 h ([M]/[I] = 100; [lactide] = 0.2 M in toluene). A conversion of 84% was achieved with a selectivity of 96%. M_n = 11 200, PDI = 1.06, and T_m = 149 °C. Because a lower temperature afforded no increase in selectivity, all subsequent reactions were performed at 70 °C.

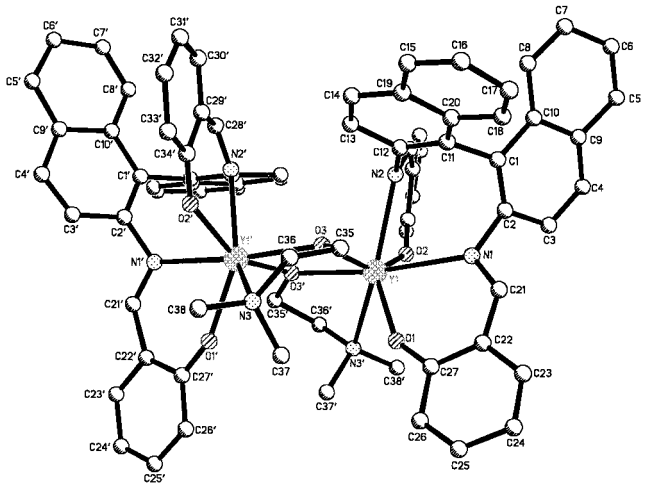

Figure 4. X-ray crystal structure of (*R*)-**5**.

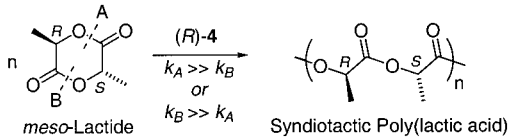

Figure 5. Synthesis of syndiotactic PLA.

Table 1. Polymerization of *meso*-Lactide with (*R*)-**4**[a]

time (h)	conversion[b] (%)	P_r[c] (%)	M_n[d] ($\times 10^{-3}$)	MWD[d]	T_g[e] (°C)	T_m[e] (°C)
5	46	95	6.28	1.05	38.5	153
11	62	95	10.69	1.05	43.6	153
15	71	94	11.98	1.05	45.8	151
20	81	96	12.26	1.04	47.3	149
30	90	96	14.39	1.06	44.0	149
40	92	96	15.44	1.06	50.7	149

[a] [*meso*-LA]/[(*R*)-**4**] = 100; T_{rxn} = 70 °C; [*m*-LA] = 0.2 M in toluene. [b] Determined via integration of the methyl resonances of *m*-LA and PLA ($CDCl_3$, 300 MHz). [c] P_r is the probability of racemic linkages between monomer units and is determined from the methine region of the homonuclear decoupled ^{1}H NMR spectrum. [d] Determined by gel permeation chromatography, calibrated with polystyrene standards in tetrahydrofuran. [e] Determined by differential scanning calorimetry with a heating rate of 10 °C/min.

The low polydispersities and the linear correlation ($r^2 = 0.99$) between M_n and conversion are indicative of a living polymerization as well as a single type of reaction site (Figure 6).[45]

According to enantiomorphic site control statistics, poly(lactic acid)s derived from both *rac*- and *meso*-lactide can exhibit five tetrad sequences (Table 2). The relative proportions of the tetrad sequences depend on the extent to which the catalyst controls racemic (*r*-dyad) and meso (*m*-dyad) placement of monomer units.[46] In the case of *meso*-lactide polymerization, the parameter α is the probability that a given enantiomer of a catalyst opens *meso*-lactide at one of the enantiotopic acyl−oxygen groups. As shown in Figure 5, *meso*-lactide has two enantiotopic acyl−oxygen sites that can be ring-opened by (*R*)-**4**; α is then equal to $k_A/(k_A + k_B)$. When α approaches 0 or 1, the polymer formed is highly syndiotactic, while atactic polymer forms when α is 0.5.

(45) This assumes that if multiple active species are present, they do not exchange polymer chains on a time scale that is faster than propagation, and they exhibit different rates of polymerization.

(46) We prefer to use the standard *m*/*r* nomenclature described by Bovey (Bovey, F. A.; Mirau, P. A. *NMR of Polymers*; Academic Press: San Diego, 1996) although it should be noted that the PLA literature often contains the *i*/*s* notation (*i* = isotactic ("*m*"), *s* = syndiotactic ("*r*")).

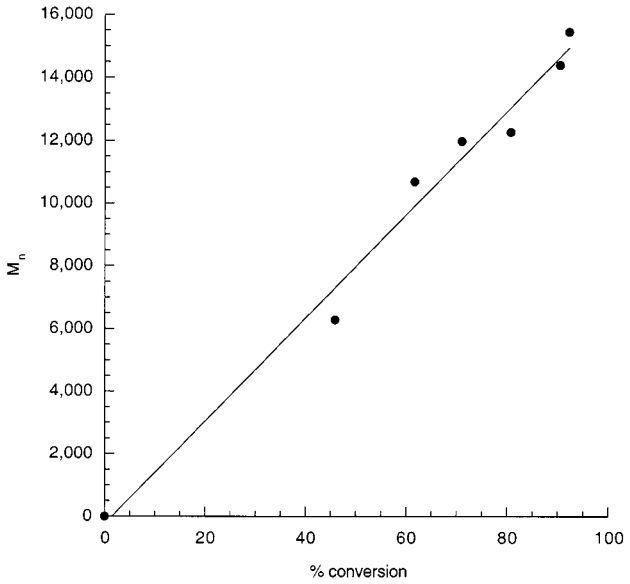

Figure 6. PLA M_n (versus polystyrene standards) as a function of conversion using *meso*-lactide and (*R*)-**4** (toluene, 70 °C, [LA]/[Al] = 100).

Table 2. Tetrad Probabilities Based on Enantiomorphic Site Control Statistics[a]

	probability	
tetrad	*meso*-lactide	*rac*-lactide
mmm	0	$[\alpha^2 + (1-\alpha)^2 + \alpha^3 + (1-\alpha)^3]/2$
mmr	0	$[\alpha^2(1-\alpha) + \alpha(1-\alpha)^2]/2$
rmm	0	$[\alpha^2(1-\alpha) + \alpha(1-\alpha)^2]/2$
rmr	$[\alpha(1-\alpha) + \alpha(1-\alpha)]/2$	$[\alpha^2(1-\alpha) + \alpha(1-\alpha)^2]/2$
mrm	$[\alpha^2(1-\alpha) + \alpha(1-\alpha)^2]/2$	$[\alpha(1-\alpha) + \alpha(1-\alpha)]/2$
rrm	$[\alpha^2(1-\alpha) + \alpha(1-\alpha)^2]/2$	0
mrr	$[\alpha^2(1-\alpha) + \alpha(1-\alpha)^2]/2$	0
rrr	$[\alpha^2 + (1-\alpha)^2 + \alpha^3 + (1-\alpha)^3]/2$	0

[a] α is the probability that a given enantiomer of a catalyst opens lactide at one of its two enantiotopic acyl−oxygen sites.

The tacticity of the polymers prepared with (*R*)-**4** was determined by inspection of the homonuclear decoupled ^{1}H NMR spectrum of the methine region (Figure 7). Peak identities were based on assignments previously reported.[47−50] ^{1}H NMR analysis proves that the polymers formed were highly syndiotactic as evidenced by the large *rrr* tetrad peak. In addition, a small *rmr* impurity peak is observed. Assuming an enantiomorphic site control mechanism (vide infra), *rrm*, *mrm*, and *mrr* tetrads must also be present due to the *-RSRSSRRSRS-* defect sequences, but are too small to be visible due to near chemical shift equivalence with the syndiotactic *rrr* tetrad peak. Further evidence for a high level of syndiotacticity is the presence of isolated absorptions in the ^{13}C NMR at δ 169.2, 69.3, and 16.3 ppm. Close inspection of the ^{13}C NMR in the methine region (Figure 8) reveals small peaks corresponding to the tetrad impurities noted above. The presence of the *mrm* tetrad as well as the [*rrm*]:[*mrm*]:[*mrr*]:[*rmr*] contents of approximately 1:1:1:2 confirm that the reaction occurs via an enantiomorphic

(47) Thakur, K. A. M.; Kean, R. T.; Hall, E. S.; Kolstad, J. J.; Lindgren, T. A.; Doscotch, M. A.; Siepmann, J. I.; Munson, E. J. *Macromolecules* **1997**, *30*, 2422−2428.

(48) Thakur, K. A. M.; Kean, R. T.; Hall, E. S.; Kolstad, J. J.; Munson, E. J. *Macromolecules* **1998**, *31*, 1487−1494.

(49) Thakur, K. A. M.; Kean, R. T.; Zell, M. T.; Padden, B. E.; Munson, E. J. *Chem. Commun.* **1998**, 1913−1914.

(50) Chisholm, M. H.; Iyer, S. S.; McCollum, D. G.; Pagel, M.; Werner-Zwanziger, U. *Macromolecules* **1999**, *32*, 963−973.

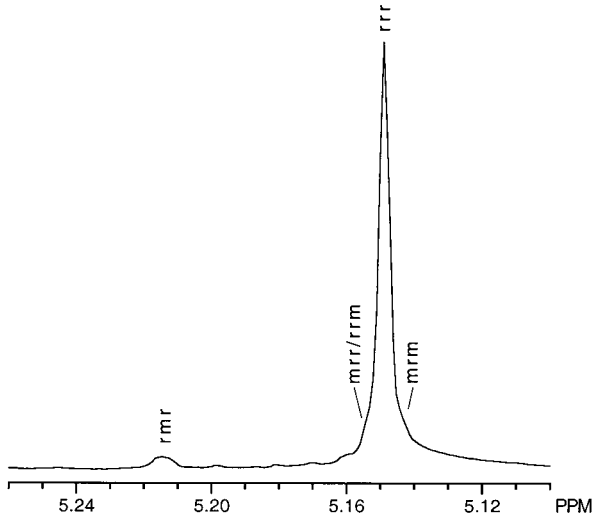

Figure 7. Homonuclear decoupled ^{1}H NMR spectrum of the methine region of PLA prepared with (*R*)-**4**/*meso*-lactide at 70 °C for 40 h (500 MHz, $CDCl_3$).

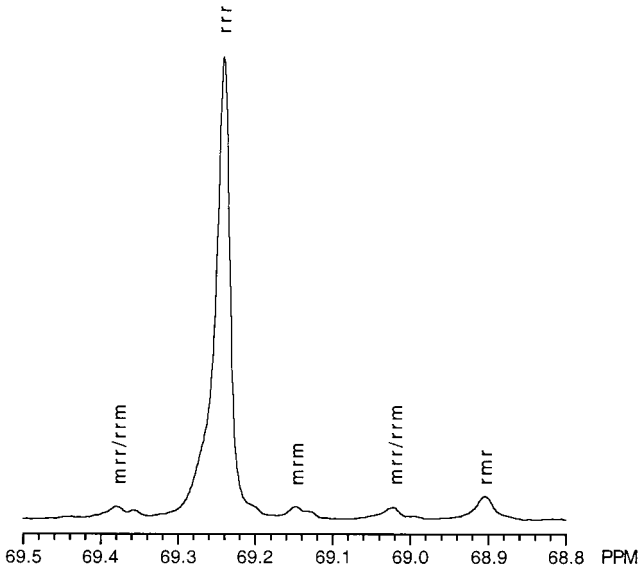

Figure 8. ^{13}C NMR spectrum of the methine region of syndiotactic PLA prepared with (*R*)-**4**/*meso*-lactide at 70 °C (75 MHz, $CDCl_3$).

site control mechanism. Comparison of the intensity of the *rmr* tetrad to the *rrr* tetrad in the homonuclear decoupled ^{1}H NMR reveals $\alpha = 0.96$ (polymer formed at 70 °C in toluene for 40 h) when tetrad intensities are fit using the enantiomorphic site model (Table 2). Therefore, the selectivity of the reaction is 96%, or in other words, 96% of the time the catalyst chooses one enantiotopic acyl−oxygen site of the lactide monomer over the other. Due to the high degree of stereoregularity, syndiotactic PLA is crystalline. Following annealing at 95 °C for 60 min, the polymer exhibits a glass-transition temperature (T_g) of approximately 45 °C, and a peak melting temperature (T_m) as high as 153 °C. Although microstructural analysis of the ^{1}H NMR spectrum (Figure 7) shows that (*R*)-**4** forms highly syndiotactic PLA from *meso*-lactide, it is not possible to determine which enantiotopic acyl−oxygen bond of the monomer is opened with the (*R*)-enantiomer of the catalyst (Figure 5). Interestingly, selective opening at *either* site produces the same syndiotactic polymer (neglecting end groups); thus, the reaction is a rare example of the polymerization of a *meso*-

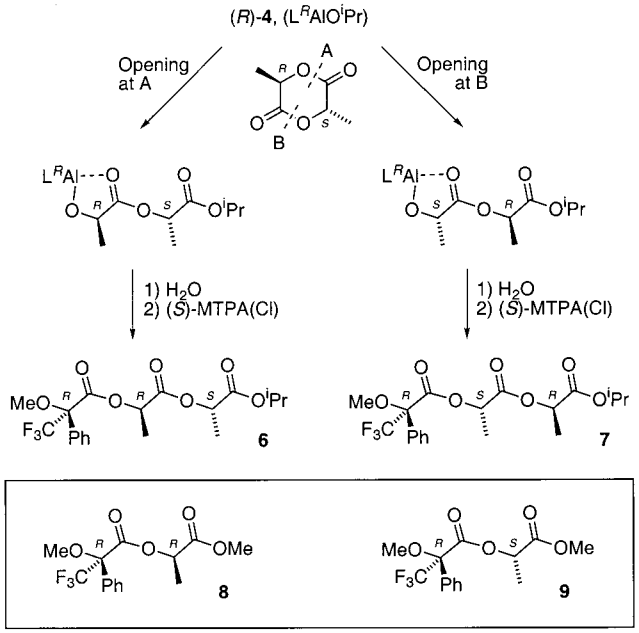

Figure 9. *meso*-Lactide adducts **6** and **7** and Mosher ester models **8** and **9** for the ring-opening site determination experiment. (Note that the labeling of the MTPA auxiliary changes from *S*- to *R*-stereochemistry upon ester formation due to a change in the CIP ordering; the absolute stereochemistry is constant.)

monomer with a chiral catalyst where an achiral polymer is produced (the polymer is however cryptochiral if the end groups are taken into consideration[51]). Since the absolute configuration of the opened site provides valuable information concerning the mechanism of stereocontrol, we decided to investigate the stereochemistry of the ring-opening process. Complex (*R*)-**4** was reacted with approximately 1 equiv of *meso*-lactide; following hydrolysis of the resultant product, (*S*)-(+)-α-methoxy-α-(trifluoromethyl)phenylacetyl chloride [(*S*)-MTPA(Cl)] was added to produce the Mosher ester (Figure 9).[52,53] Following column chromatography, a diastereomeric mixture of the possible Mosher esters of the ring-opened adducts (**6**, **7**) were isolated and analyzed using ^{1}H NMR spectroscopy (Figure 10). Using the model compounds **8** and **9** (Figure 9), which have Mosher methoxy shifts at δ 3.65 and 3.57, respectively, we have assigned the minor peak at δ 3.65 to **6** and the major peak at δ 3.55 to **7**. Therefore, (*R*)-**4** opens *meso*-lactide preferentially at site B (Figure 9) to yield a syndiotactic polymer with an (*S*)-lactic acid unit at the active end bound to the metal. The relative ratio **6**:**7** is 3:97, which agrees well with the observed selectivity of (*R*)-**4** for the polymerization of *meso*-lactide (4:96).[54] Since the stereoselectivity of insertion of *meso*-lactide into the achiral isopropoxide of (*R*)-**4** is not significantly enhanced or diminished, we propose that chain-end effects are not significant in these systems. On the basis of the observed absolute configuration of the ring-opening of *meso*-lactide using (*R*)-**4**, we propose a mechanism for ring-opening that embodies this information (Figure 11).

Polymerization of *meso*-Lactide Using a Racemic Catalyst. The polymerization of *meso*-lactide with optically active **4**

(51) Mislow, K.; Bickart, P. *Isr. J. Chem.* **1976/77**, *15*, 1−6.
(52) Dale, J. A.; Dull, D. L.; Mosher, H. S. *J. Org. Chem.* **1969**, *34*, 2543−2549.
(53) Dale, J. A.; Mosher, H. S. *J. Am. Chem. Soc.* **1973**, *95*, 512−519.
(54) The corresponding experiment with (*S*)-**4** confirmed ring-opening at site A to form an *R*-chain end with a similar high selectivity.

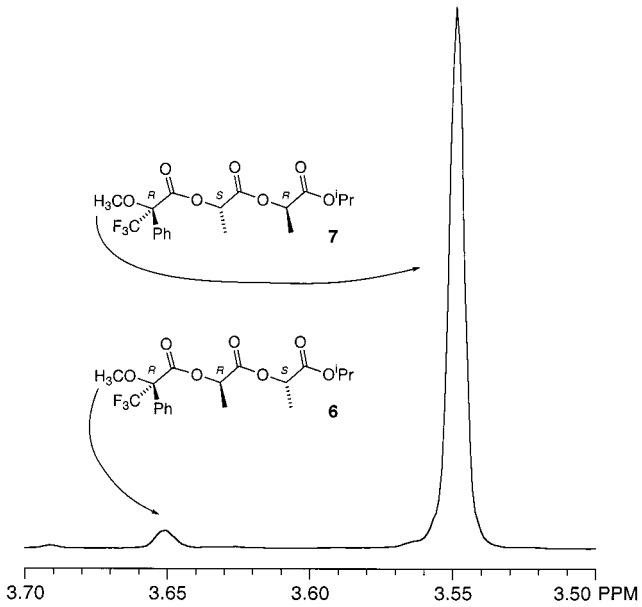

Figure 10. ^{1}H NMR spectrum of the Mosher group methoxy region of the *meso*-lactide ring-opened adducts using (*R*)-**4** (300 MHz, $CDCl_3$).

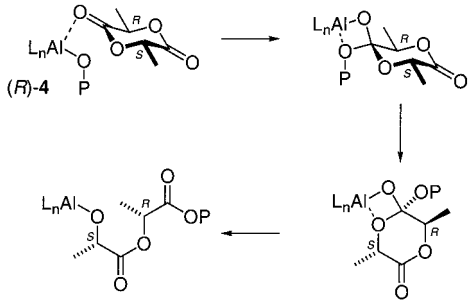

Figure 11. Proposed mechanism of ring-opening of *meso*-lactide using (*R*)-**4**.

afforded achiral syndiotactic PLA. Typically, a racemic catalyst is much less expensive than either of its optically active components. Therefore, we investigated the reaction of *meso*-lactide with *rac*-(SalBinap)AlO^{i}Pr to determine whether syndiotacticity requires optically active catalyst. After 40 h at 70 °C the reaction of *rac*-**4** with *meso*-lactide proceeded to 98% conversion ([LA] = 0.212 M in toluene, [LA]/[*rac*-**4**] = 106). Gel-permeation chromatography (GPC) revealed a M_n = 13,600 (theoretical M_n = 15,000) and a MWD of 1.07. The polymer was amorphous and exhibited a T_g = 43.2 °C.

The most notable feature of the reaction using the racemic catalyst is that the polymer formed was unexpectedly heterotactic, where 80% of the linkages formed during the polymerization occurred between lactic acid units of identical stereochemistry (Figure 12). The methine region of the homonuclear decoupled ^{1}H NMR spectrum of the polymerization of *meso*-lactide by *rac*-**4** is shown in Figure 13. The peaks were assigned to the appropriate tetrads in accordance with the correlations established in the literature.[47−50] The major tetrad peaks correspond to those of the *mrm* and *rmr* tetrads, indicative of the heterotactic -*RRSSRRSS*- sequence of the polymer (Figure 13). Also present were the *rrr*, *rrm*, and *mrr* tetrad impurities, corresponding to a -*RSSRRSRSSRRS*- defect sequence.[55] We propose a polymer exchange mechanism to account for the formation of this heterotactic microstructure, whereby each individual polymer chain effectively switches between enantiomeric aluminum centers before insertion of a subsequent monomer unit (Figure 14). Currently, we cannot rule out the possibility of a bimetallic active species bearing enantiomeric ligands, although current kinetic data is consistent with a monomeric enchainment mechanism (vide infra). The mechanism proposed in Figure 14 is conceptually related to an ancillary ligand exchange mechanism reported by Brookhart and Wagner to account for the formation of a syndiotactic polyketone when an optically active complex was used in the presence of an equivalent of enantiomeric ligand.[56] The detailed nature of the switching process is not clear, however we propose exchange through μ-alkoxide or [L_nAl^+][OP^-] ionic species result in polymer transfer. We have found that added alcohol results in an "immortal" polymerization[5] (through rapid alcoholysis new polymer chains grow, resulting in decreased overall molecular weight for a given [LA]/[Al] ratio). Thus the possibility that trace protic impurities shuttle chains between enantiomeric aluminum centers cannot be ruled out at the current time. By studying the absolute stereochemistry of ring opening, we know that the (*R*)- and (*S*)-***4*** open *meso*-lactide to place *S*- and *R*-stereocenters, respectively, at the growing end of the polymer chain, respectively. Molecular modeling suggests that the (*R*)-catalyst prefers an *R*-center (and the (*S*)-catalyst prefers an *S*-center), assuming a C_2-symmetric ligand configuration. If polymer exchange is rapid, then the differences between the

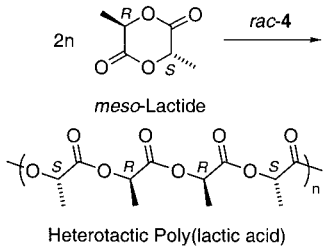

Figure 12. Synthesis of heterotactic PLA.

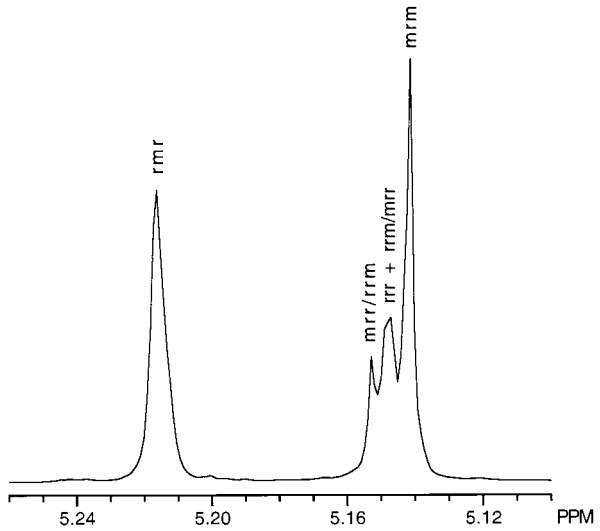

Figure 13. Homonuclear decoupled ^{1}H NMR spectrum of the methine region of heterotactic PLA prepared with *rac*-**4**/*meso*-lactide at 70 °C (500 MHz, $CDCl_3$).

(55) Although the ^{13}C NMR spectrum shows an approximate 1:1:1 ratio of the *rrr*, *mrr*, and *rrm* tetrads, the ^{1}H NMR shows a 2:1 ratio of what has previously been assigned as the *rrr* and *rrm*+ *mrr* tetrads, respectively. Since the ratio should be 1:2, we propose that either the *rrm* or *mrr* tetrad must exhibit chemical shift equivalence with the *rrr* tetrad for this polymer.

(56) Brookhart, M.; Wagner, M. I. *J. Am. Chem. Soc.* **1996**, *118*, 7219−7220.

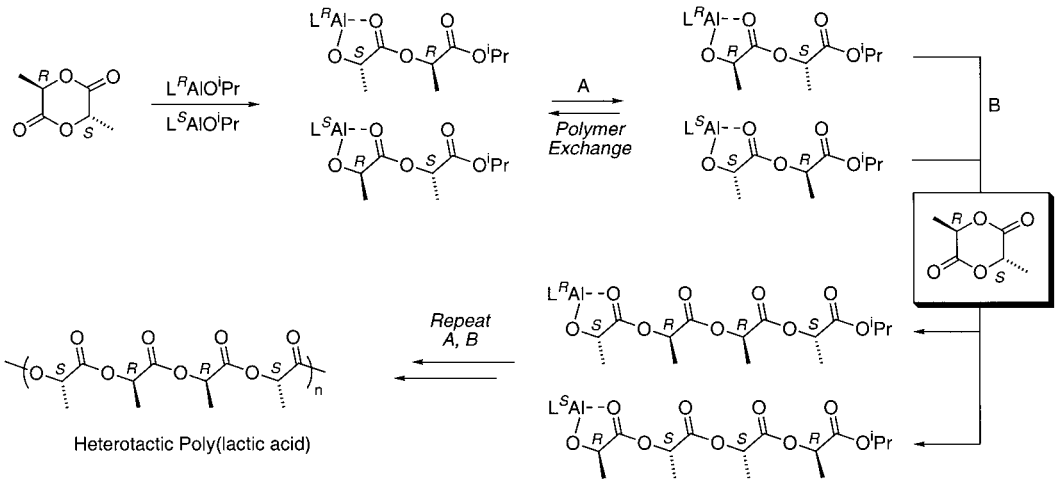

Figure 14. Proposed mechanism of heterotactic PLA formation.

standard free energies of the transition states leading to syndiotactic and heterotactic PLA will determine stereochemistry. Hence we propose a polymer exchange/insertion sequence to account for the heterotactic structure of the polymer (A, B; Figure 14). The exact nature of stereochemical control is clearly very complex, and will be the subject of further study in our lab.

Polymerization of *rac*-Lactide Using a Racemic Catalyst. Isotactic PLA exhibits a peak melting temperature of 170−180 °C.[57] However, when poly[(*R*)-(lactic acid)] and poly[(*S*)-(lactic acid)] are mixed, cocrystallization occurs and the T_m of the resulting stereocomplex is 230 °C.[58−61] This observation motivates an attempt to use *rac*-lactide for the preparation of isotactic PLA directly from *rac*-lactide, where both enantiomers of the monomer are simultaneously incorporated into poly(*R*) segments and poly(*S*) segments. Stereocomplex PLA is an attractive target for several reasons, including the enhancement in melting temperature and the low cost of the *rac*-lactide monomer.

The polymerization of *rac*-lactide with (*R*)-**2** afforded a tapered stereoblock PLA with a T_m much lower than the theoretical maximum of 230 °C.[8] A gradient of stereogenic centers in the main chain was the apparent cause. One method of circumventing this problem is to sequentially polymerize (*R*,*R*)-lactide and then (*S*,*S*)-lactide with an achiral, living initiator.[57] However, this strategy suffers from the fact that (*R*,*R*)-lactide is much more expensive than the (*S*,*S*)-enantiomer. An alternate approach is to employ a more selective catalyst to effect the kinetic resolution of *rac*-lactide (i.e., a catalyst with a propagation rate constant for the preferred enantiomer that is much higher than the corresponding rate constant for the unpreferred enantiomer). The disadvantage of this strategy is that an increase in the ratio of these rate constants will dramatically lengthen the reaction time, if the rate of enchainment of the preferred enantiomer is held constant.

An even more formidable synthetic accomplishment would be the polymerization of *rac*-lactide to form separate isotactic poly[(*R*)-(lactic acid)] and poly[(*S*)-(lactic acid)] chains in a "one-pot" reaction. On the basis of our previous findings, we speculated that this objective might be met with *rac*-(SalBinap)-AlO^{i}Pr. It was expected that (*R*)-**4** would produce pure chains of (*R*)-lactide, (*S*)-**4** would produce pure chains of (*S*)-lactide, and the chains would cocrystallize to form a high-melting stereocomplex. Initial experiments on the polymerization of *rac*-lactide with *rac*-(SalBinap)AlO^{i}Pr yielded highly crystalline, predominantly isotactic material, apparently consistent with the desired goal of simultaneously forming pure isotactic (*R*)-PLA and (*S*)-PLA (Figure 15). In fact, during the course of our work Baker and Smith reported exactly this finding, confirming our original results.[19] However, on the basis of the observation of polymer exchange during the polymerization of *meso*-lactide using *rac*-**4**, we decided to investigate the detailed microstructure of the polymer formed from *rac*-lactide/*rac*-**4** with the expectation that the polymer might not consist of enantiomerically enriched chains.[19] In fact, further examination of our data revealed the formation of a stereoblock PLA instead (Figure 15).

The methine region of the homonuclear decoupled ^{1}H NMR spectrum of the polymerization of *rac*-lactide by *rac*-**4** is shown in Figure 16. The peaks were assigned to the appropriate tetrads in accordance with the literature.[47−50] The *mmm* tetrad, diagnostic of isotacticity, is the predominant peak in the spectrum. However, it is the defect tetrads that reveal the true structure of the polymer, and provide valuable information about the mechanism of stereocontrol. The *rmm*, *mmr*, and *mrm* tetrads are all present in approximately equal intensity, with an additional small *rmr* peak near 5.22 ppm. If the polymer sample consisted of isotactic PLA, where each chain was made by one molecule of

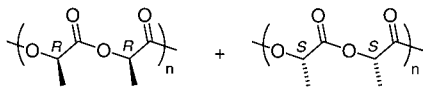

Stereocomplex Poly(lactic acid)
Isotactic Poly((*R*)-lactic acid) / Isotactic Poly((*S*)-lactic acid)

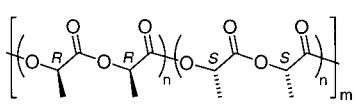

Stereoblock Isotactic Poly(lactic acid)

Figure 15. Stereocomplex and stereoblock PLAs.

(57) Spinu, M.; Jackson, C.; Keating, M. Y.; Gardner, K. H. *J. Macromol. Sci., Pure Appl. Chem.* **1996**, *A33*, 1497−1530.
(58) Ikada, Y.; Jamshidi, K.; Tsuji, H.; Hyon, S. H. *Macromolecules* **1987**, *20*, 904−906.
(59) Loomis, G. L.; Murdoch, J. R. (Dupont). U.S. Patent 4,719,246, 1988.
(60) Loomis, G. L.; Murdoch, J. R. (Dupont). U.S. Patent 4,800,219, 1989.
(61) Tsuji, H.; Ikada, Y. *Polymer* **1999**, *40*, 6699−6708.

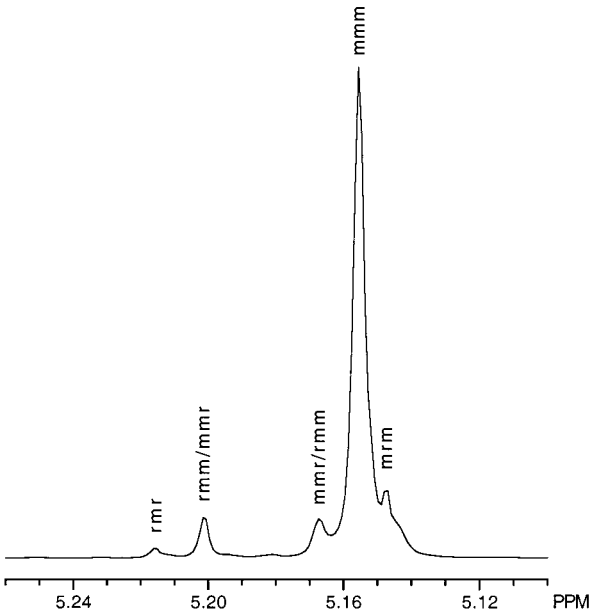

Figure 16. Homonuclear decoupled ^{1}H NMR spectrum of the methine region of PLA prepared with *rac*-**4**/*rac*-lactide at 70 °C (500 MHz, $CDCl_3$).

4, the sequences of the chain would be -*RRRRRRSSRRRRRR*-/-*SSSSSSRRSSSSSS*- due to an enantiomorphic site control of stereochemistry. Thus, in the Bovey nomenclature, sequences of the type -*mmrmrmm*- would be present, with *mmr*, *mrm*, *rmr*, and *rmm* tetrads in a predicted 1:2:1:1 ratio. Due to the inordinately small size of the *rmr* tetrad, this polymer sample cannot be a stereocomplex of highly enantiomerically enriched chains (Figure 15). An alternate proposal is that the polymer is in fact a stereoblock PLA with alternating blocks of (*R*)-lactide and (*S*)-lactide in the main chain. Such a polymer would have -*RRRRRRSSSSSS*- sequences in the main chain, and would still have the capability of adopting a stereocomplex morphology in the solid state. In the Bovey designation sequences of the type -*mmmmrmmmm*- would be present, with *mmr*, *mrm*, and *rmm* tetrads in a predicted 1:1:1 ratio (*rmr* tetrad absent). Therefore, we propose that the structure of the polymer formed from *rac*-lactide and *rac*-**4** is best represented as a stereoblock PLA (Figure 15). The presence of a small *rmr* peak suggests that a minimal amount of the unpreferred enantiomer is incorporated into the chain at a level consistent with the selectivity of (*R*)-**4** for (*R*,*R*)- versus (*S*,*S*)-lactide.

A statistical model was used to simulate the spectrum of the PLA formed with both stereoerror and the exchange processes occurring to produce stereochemical defects. A site control selectivity (α) of 0.98 and stereoblocks containing an average of 11 units (n) of enantiomerically pure lactide were shown to minimize the difference between the simulation output spectrum and experimental spectrum. Hence, we conclude that the best representation of the polymer formed from *rac*-lactide and *rac*-**4** is a stereoblock polymer, containing consecutive sequences of *R*- and *S*-centers.

We propose a mechanism of stereocontrol (Figure 17) that is conceptually related to that for *meso*-lactide shown in Figure 14. The predominant ring-opening event is reaction of (*R*)-**4** and (*S*)-**4** with (*R*)-lactide and (*S*)-lactide, respectively (A). Eventually, due to the modestly higher activation energy of reacting with the disfavored lactide stereoisomer, polymer exchange occurs and the wrong enantiomer of lactide is incorporated (B, C). At this point, propagation resumes with the favored lactide stereoisomer, creating a stereoblock structure. An alternative interpretation of the data is that, prior to polymer exchange, the disfavored lactide is enchained. This is followed by polymer exchange where the propagation resumes with the favored lactide enantiomers. Since both pathways give the same polymer, neither can be ruled out at the current time.

The stereoblock PLA prepared from the reaction of *rac*-lactide and *rac*-**4** at 70 °C ([*rac*-lactide]/[Al] = 100) exhibited a peak T_m at 179 °C, which was higher than that of isotactic poly[(*R*)-(lactic acid)] or poly[(*S*)-(lactic acid)]. This is strong evidence that these block copolymers adopt a stereocomplex morphology in the solid state, and due to the shorter runs of enantiomerically pure blocks in the main chain, the melting points are lower than a 1:1 mix of the enantiopure homopolymers. The polymer was analyzed by GPC, revealing a M_n = 22 600 and a molecular weight distribution of 1.09. The polymerization exhibits living behavior, as evidenced by the correlation between the predicted and observed molecular weights and the narrow MWD. In addition, the narrow MWD suggests that no significant transesterification occurs. Indeed, for enantiomerically pure isotactic chains to form (Figure 15), transesterification cannot take place. It should be noted that, in our proposed mechanism, a type of transesterification does occur, but since the chains are not lengthened or shortened, the molecular weight distribution remains monodisperse.

Kinetics of Lactide Polymerization with (SalBinap)AlO^{i}Pr. To determine the relative rates of reaction for the polymerization of lactide with (SalBinap)AlO^{i}Pr, a series of consecutive reactions was run for each of the following monomer−initiator combinations: (i) (*S*,*S*)-lactide + (*S*)-(SalBinap)AlO^{i}Pr, (ii) *meso*-lactide + *rac*-(SalBinap)AlO^{i}Pr, (iii) *rac*-lactide + *rac*-(SalBinap)AlO^{i}Pr, and (iv) *meso*-lactide + (*R*)-(SalBinap)AlO^{i}Pr. All reactions were run under the same conditions at 70 °C in toluene ($[LA]_o$ = 0.2 M; [Al] = 0.002 M; [LA]/[Al] = 100). Lactide conversion with time was monitored by ^{1}H NMR spectroscopy until monomer consumption reached 90%. In each case, first-order kinetics in monomer were observed.[62] At high conversion of monomer, slight deviation from first-order behavior occurs, which is proposed to be due to the formation of cyclic species (discovered using MALDI-TOF MS).[63−65] Therefore, data collected at long reaction times were not used. The polymerization of lactide by (SalBinap)AlO^{i}Pr obeys the first-order rate law

$$-\mathrm{d[LA]}/\mathrm{d}t = k_{app}[\mathrm{LA}]^1 \qquad (1)$$

where $k_{app} = k_p[\mathrm{Al}]^x$, and where k_p is the propagation rate constant. To determine the order in aluminum, ln k_{app} versus ln [Al] was plotted for the polymerization of *meso*-lactide with (*R*)-**4** at [LA]/[Al] = 50, 75, and 100.[62] At higher [LA]/[Al] ratios, the kinetic data were irreproducible. From this plot, the order in initiator (slope) is 1.1 ± 0.3. Due to the limited data, though, the order in initiator must be considered preliminary.

(62) See the Supporting Information.
(63) Spassky, N.; Simic, V.; Montaudo, M. S.; Hubert-Pfalzgraf, L. G. *Macromol. Chem. Phys.* **2000**, *201*, 2432−2440.
(64) Spassky, N.; Simic, V.; Hubert-Pfalzgraf, L. G.; Montaudo, M. S. *Macromol. Symp.* **1999**, *144*, 257−267.
(65) Montaudo, G.; Montaudo, M. S.; Puglisi, C.; Samperi, F.; Spassky, N.; LeBorgne, A.; Wisniewski, M. *Macromolecules* **1996**, *29*, 6461−6465.

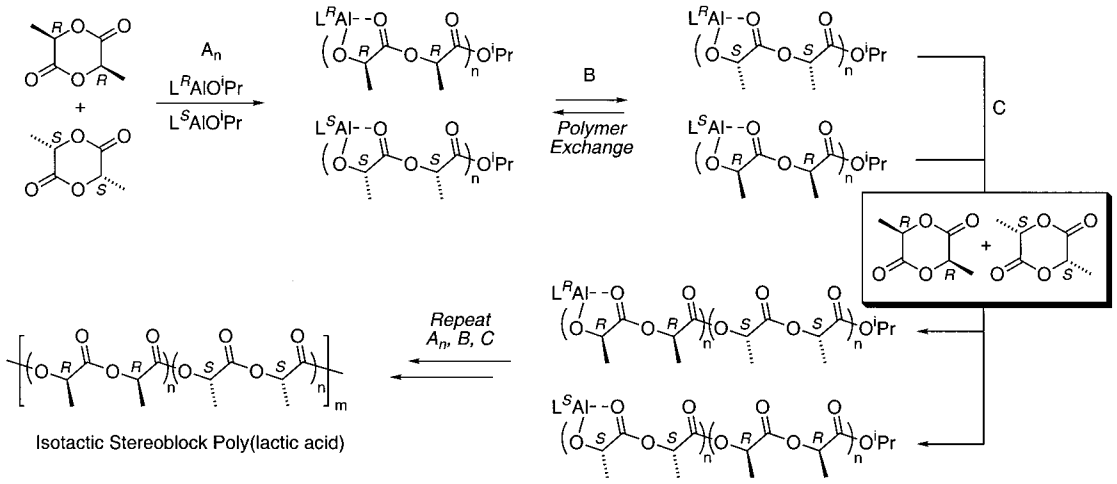

Figure 17. Proposed mechanism of stereoblock PLA formation.

Therefore, we currently propose the polymerization of *meso*-lactide by (*R*)-**4** follows an overall kinetic law of the form

$$-\mathrm{d[LA]}/\mathrm{d}t = k_{\mathrm{p}}[\mathrm{Al}][\mathrm{LA}] \qquad (2)$$

At the current time we cannot rule out the presence of an alkoxide-bridged bimetallic resting state of the catalyst that reacts with lactide in a bimetallic pathway that would also yield first-order kinetics with respect to aluminum. Due to the stability of the chelate formed by the polymer chain end with the aluminum center (Figure 11), we favor a monomeric species as the active catalyst.

The first-order rate constant (k_{app}) for the polymerization of (*S*,*S*)-lactide with (*S*)-**4** to form isotactic PLA is the largest of those studied (5.5×10^{-3} min^{-1}). Therefore, the formation of isotactic PLA has the fastest rate of reaction relative to the other systems. The system with the second fastest relative rate was the reaction of *meso*-lactide with *rac*-**4** to form heterotactic PLA (4.4×10^{-3} min^{-1}). The relative rate of reaction of *rac*-lactide with *rac*-**4** to form stereoblock PLA (2.1×10^{-3} min^{-1}) was approximately half the rate of formation of isotactic PLA from (*S*)-**4** and the preferred enantiomer. The magnitudes of these rate constants are reasonable considering that, in the case of the polymerization of (*S*,*S*)-lactide with (*S*)-**4**, all monomer molecules may be ring-opened by all catalyst molecules. In contrast, only half of the monomer molecules may be ring-opened by each catalyst enantiomer in the polymerization of *rac*-lactide with *rac*-**4**.

The polymerization of *meso*-lactide with (*R*)-**4** to form syndiotactic poly(lactic acid) exhibits a k_{app} of 2.0×10^{-3} min^{-1}. This is approximately half the rate of formation of heterotactic PLA from *meso*-lactide with *rac*-**4**. This result is reasonable on the basis of the fact that (*R*)-**4** can only open *meso*-lactide at one acyl−oxygen. In contrast, *rac*-**4** has the kinetic advantage of rapid polymer exchange, followed by a lower energy pathway for ring-opening after the exchange occurs.

Summary and Conclusions

The synthesis of chiral aluminum and yttrium alkoxides and their application for lactide polymerization is reported. Although enantiomerically pure yttrium complex (*R*)-**5** did not effect stereocontrol in the polymerization of either *meso*- or *rac*-lactide, homochiral (*R*)-**4** was found to exhibit excellent stereocontrol in a range of lactide polymerizations. Enantiomerically pure (*R*)-**4** polymerizes *meso*-lactide to syndiotactic PLA with an enantiotopic ring-opening selectivity of 96%. Interestingly, *rac*-**4** polymerizes *meso*-lactide to heterotactic PLA. On the basis of the absolute stereochemistry of ring-opening of *meso*-lactide using (*R*)-**4**, a polymer exchange mechanism is proposed to account for the tacticity of this polymer. With this information in mind we reinvestigated the polymer made from *rac*-lactide using (*R*)-**4**. Instead of producing the expected stereocomplex PLA consisting of enantiomerically pure strands of isotactic polymer, an isotactic stereoblock PLA was produced. We propose this novel microstructure again results from a polymer exchange mechanism, where runs of enantiomerically pure lactide are interrupted by periodic changes in stereochemistry due to interchange between enantiomeric catalyst species.

Due to the growing importance of lactic acid polymers in a range of biomedical, agricultural, and packaging applications, the results reported here are significant in that new routes to PLA architectures are now available. Subsequent work in our group will center on the study of the physical and mechanical properties of these polymers. However, perhaps the most important implication of the current work is that single-site catalysts offer new opportunities for microstructural control if new reaction pathways are accessed through catalyst design and control of reaction conditions. Our future research will be directed toward increasing the mechanistic complexity of polymerization catalysts to produce previously unattainable polymer architectures.

Experimental Section

General Considerations. All reactions with air- and/or water-sensitive compounds were carried out under dry nitrogen using a MBraun Labmaster drybox or standard Schlenk line techniques. NMR spectra were recorded on Bruker AF300 (^{1}H, 300 MHz; ^{13}C, 75 MHz) and Varian UNITY 500 (^{1}H, 500 MHz; ^{13}C, 125 MHz) spectrometers, and referenced versus shifts of solvents containing residual protic impurities. For ^{1}H NMR, coupling constants *J* are given in hertz. Gel permeation chromatography (GPC) analyses were carried out using a Waters instrument (M510 pump, U6K injector) equipped with Waters UV486 and Milton Roy differential refractive index detectors, and four 5 μm PL Gel columns (Polymer Laboratories; 100, 500, and 1000 Å, and mixed C porosities) in series. The GPC columns were eluted with tetrahydrofuran at 45 °C at 1 mL/min and were calibrated using 23 monodisperse polystyrene standards. Crystallographic data were col-

lected using a SMART CCD area detector system (Mo Kα, $\lambda = 0.71073$ Å), and frames were integrated with the Siemens SAINT program. DSC analyses were performed on a Seiko DSC 220C instrument using EXSTAR 6000 processing software. The measurements were made in aluminum crimped pans under nitrogen with a heating rate of 10 °C/min. Reported values originate from the second heating scan. Elemental analysis was performed by Galbraith Laboratories in Knoxville, TN. High-resolution fast atom bombardment mass spectra were obtained in the Mass Spectrometry Laboratory, School of Chemical Sciences, University of Illinois. The 70-SE-4F mass spectrometer was purchased in part with funds from the National Institute of General Medical Sciences (Grant GM 27029).

Materials. Toluene was distilled from sodium benzophenone ketyl, hexanes from $LiAlH_4$, and CH_2Cl_2 from CaH_2; residual gases were removed using a freeze−pump−thaw technique. *meso*-Lactide was synthesized as described in the literature[66] and was determined to be greater than 99% pure by ^{1}H NMR and GC analysis. *rac*-Lactide was purchased from Purac and was sublimed prior to use. Aluminum isopropoxide was distilled under vacuum immediately before use.[67] The ligands (*R*)-(SalBinap)H_2 [(*R*)-**1**] and (*S*)-(SalBinap)H_2 [(*S*)-**1**] were synthesized according to a published procedure.[41] All other chemicals were commercially available and used as received.

[(*R*)-SalBinap]$_2$Al$_2$(OMe)$_2$ [(*R*)-3]. In a drybox, a Schlenk tube was loaded with the chiral Schiff base (*R*)-**1** (0.300 g, 0.609 mmol). Toluene (5 mL) was added, and the ligand dissolved upon heating to 70 °C. A toluene solution of $AlEt_3$ (1.9 M, 0.320 mL, 0.608 mmol) was added at room temperature. The reaction was stirred at room temperature for 4 h to afford (*R*)-(SalBinap)AlEt, which was then stirred in excess methanol (5 mL) for 3 h. The insoluble yellow solid (*R*)-**2** was filtered off (0.210 g). The product (*R*)-**3** formed as large colorless crystals from the methanol mother liquors (0.099 g, 30% yield). ^{1}H NMR ($CDCl_3$, 300 MHz): δ 9.01 (2H, d, $J = 8.6$), 7.81 (2H, s), 7.55 (2H, d, $J = 8.1$), 7.50 (2H, d, $J = 9.1$), 7.32 (2H, d, $J = 8.6$), 7.22 (3H, t), 7.04−7.14 (10H, m), 6.20−6.25 (2H, m), 5.91 (2H, d, $J = 7.5$), 2.67 (3H, s). X-ray analysis of the crystals revealed that the complex exists as a bimetallic helicate.[62]

(*R*)-(SalBinap)AlO^{i}Pr [(*R*)-4]. In a glovebox, a Schlenk tube was loaded with freshly distilled aluminum isopropoxide (0.137 g, 0.671 mmol), (*R*)-**1** (0.329 g, 0.668 mmol), and toluene (10 mL). The mixture was heated to 70 °C and stirred for 2 days. The solvent was removed in vacuo, yielding a yellow solid. Despite repeated attempts, crystallization of the complex was unsuccessful. NMR clearly revealed that impurities or multiple aggregation states were present. ^{1}H NMR (tol-d_8, 300 MHz): δ 7.92 (1H, s), 7.76 (2H, d, $J = 4.3$), 7.68 (2H, t), 7.43 (4H, d, $J = 8.6$), 7.31 (4H, t), 7.18 (2H, t), 6.90−7.14 (18H, m), 6.53 (1H, d, $J = 8.6$), 6.42 (1H, d, $J = 7.5$), 6.28−6.36 (2H, m), 6.23 (2H, t), 4.08 (1H, m), 1.34 (3H, d, $J = 6.4$), 0.71 (3H, d, $J = 5.9$). Anal. Calcd for $C_{37}H_{29}AlN_2O_3$: C, 77.07; H, 5.07; N, 4.86. Found: C, 76.37; H, 5.34; N, 4.50.

(*S*)-(SalBinap)AlO^{i}Pr [(*S*)-4]. The method described for (*R*)-**4** was used for the synthesis of (*S*)-**4** from (*S*)-**1**.

[(*R*)-(SalBinap)YO(CH$_2$)$_2$NMe$_2$]$_2$ [(*R*)-5]. In a glovebox, a Schlenk tube was loaded with Y(O(CH$_2$)$_2$NMe$_2$)$_3$[43] (0.293 g, 0.829 mmol), (*R*)-(+)-**1** (0.412 g, 0.836 mmol), and toluene (50 mL). The mixture was heated to 70 °C and stirred for 1 day. The solvent was removed in vacuo, yielding a yellow solid. The product was recrystallized by dissolution in a minimum amount of methylene chloride, then layering with hexanes, and being allowed to stand for 24 h. Cannulation of solvent and drying of residual crystals in vacuo yielded [(*R*)-**5**]$_2$ (0.365 g, 66% yield). ^{1}H NMR (tol-d_8, 300 MHz): δ 8.15 (1H, s), 7.76 (2H, m), 7.54 (1H, d, $J = 7.5$), 7.2−7.4 (5H, m), 6.7−7.1 (13H, m), 3.27 (2H, m), 2.97 (2H, m), 2.55 (6H, br s), 1.59 (2H, m), 1.02 (2H, m). X-ray analysis of the crystals revealed that the complex exists as a μ-alkoxide-bridged dimer in the solid state.[62]

Polymer Synthesis. The following is a representative procedure using (*R*)-**4** and *meso*-lactide: In the drybox, (*R*)-**4** (8.0 mg, 1.4×10^{-5} mol), *meso*-lactide (0.2013 g, 1.4×10^{-3} mol), toluene (7.00 mL), and a magnetic stirbar were placed in a Schlenk tube. The system was heated to the desired temperature (50 or 70 °C), and the mixture stirred for 40 h. An aliquot was taken for percent conversion analysis by ^{1}H NMR. The solvent was removed in vacuo and the polymer dissolved in CH_2Cl_2 and precipitated from cold MeOH. The white crystalline solid was filtered and dried in vacuo to a constant weight. Yield: 0.165 g.

The following is a representative procedure using *rac*-(SalBinap)-AlO^{i}Pr (*rac*-**4**) and *rac*-lactide: In the drybox, a Schlenk tube was loaded with (*R*)-**4** as a 0.0106 M solution in toluene (0.657 mL, 0.0069 mmol), (*S*)-**4** as a 0.0117 M solution in toluene (0.592 mL, 0.0069 mmol), *rac*-lactide (0.199 g, 1.38 mmol), and toluene (6 mL). The system was heated to 70 °C and the mixture stirred for 40 h. The reaction was quenched via rapid cooling with liquid N_2. The solvent was removed in vacuo, and the polymer dissolved in CH_2Cl_2 and precipitated from cold MeOH. The white crystalline solid was isolated and dried in vacuo to a constant weight. Yield: 0.199 g.

The following is a representative procedure using *rac*-**4** and *meso*-lactide: In the drybox, a dry Schlenk tube was loaded with (*R*)-**4** as a 0.0106 M solution in toluene (0.657 mL, 0.0069 mmol), (*S*)-**4** as a 0.0117 M solution in toluene (0.592 mL, 0.0069 mmol), *meso*-lactide (0.214 g, 1.48 mmol), and toluene (6 mL). The system was heated to 70 °C and the mixture stirred for 40 h. The reaction was quenched via rapid cooling with liquid N_2. The solvent was removed in vacuo, and the polymer dissolved in CH_2Cl_2 and precipitated from cold MeOH. The white crystalline solid was isolated and dried in vacuo to a constant weight. Yield: 0.169 g.

(*R*)-2-Methoxy-2-(trifluoromethyl)phenylacetate of Isopropyl Lactoyllactate (from *meso*-Lactide/(*S*)-4) (6). In the drybox, a dry NMR tube was loaded with (*S*)-**4** (0.024 g, 0.041 mmol), toluene-d_8 (0.7 mL), and *meso*-lactide (0.0047 g, 0.033 mmol). The tube was sealed with a rubber septum, shaken, and allowed to stand at room temperature overnight. H_2O (1 μL) was added via syringe and the solution shaken. The solvent was removed in vacuo, yielding a yellow residue. Dry $CDCl_3$ (0.3 mL), dry pyridine (0.3 mL), and (*S*)-(+)-α-methoxy-α-(trifluoromethyl)phenylacetyl chloride ((*S*)-MTPA(Cl); 8.5 μL, 0.046 mmol) were added via syringe. The reaction mixture was allowed to stand overnight. The tube was removed from the drybox, and *N*,*N*-dimethyl-1,3-propanediamine (7.8 μL, 0.062 mmol) was added via syringe to react with excess (*S*)-MTPA(Cl). The solution was shaken vigorously and allowed to stand at room temperature for at least 5 min. The solution was diluted with ether (15 mL) and washed with cold 1 N HCl (3 × 10 mL), saturated Na_2CO_3 (3 × 10 mL), and saturated NaCl (3 × 10 mL). The organic phase was dried over Na_2SO_4, filtered, and concentrated in vacuo, yielding a yellow oil. The product was purified via flash chromatography (CH_2Cl_2, $R_f = 0.43$). Yield: 0.0014 g. ^{1}H NMR spectroscopic analysis revealed a 97:3 ratio of **6**:**7**. ^{1}H NMR ($CDCl_3$, 300 MHz): δ 7.60−7.63 (2H, m), 7.38−7.43 (3H, m), 5.28−5.35 (1H, m), 5.07−5.13 (1H, m), 5.01−5.06 (1H, m), 3.65 (3H, br s), 1.56 (3H, d, $J = 7.0$), 1.48 (3H, d, $J = 7.0$), 1.26 (3H, d, $J = 5.9$), 1.22 (3H, d, $J = 6.5$). HRMS (FAB): *m*/*z* 421.1473 ((M + H)$^+$, $C_{19}H_{24}O_7F_3$ requires 421.1474).

(*R*)-2-Methoxy-2-(trifluoromethyl)phenylacetate of Isopropyl Lactoyllactate (from *meso*-Lactide/(*R*)-4) (7). The method described for the synthesis of **6** from (*S*)-**4** and *meso*-lactide was used for the synthesis of **7** from (*R*)-**4** and *meso*-lactide. Yield: 0.0019 g. ^{1}H NMR spectroscopic analysis revealed a 97:3 ratio of **7**:**6**. ^{1}H NMR ($CDCl_3$, 300 MHz): δ 7.60−7.63 (2H, m), 7.38−7.43 (3H, m), 5.31−5.38 (1H, m), 4.99−5.10 (2H, m), 3.55 (3H, br s), 1.63 (3H, d, $J = 7.0$), 1.45 (3H, d, $J = 7.0$), 1.24 (3H, d, $J = 7.0$), 1.22 (3H, d, $J = 7.0$). HRMS (FAB): *m*/*z* 421.1477 ((M + H)$^+$, $C_{19}H_{24}O_7F_3$ requires 421.1474).

(66) Entenmann, G.; Bendix, D. (Boehringer Ingelheim). Ger. Offen. DE 3,820,299, 1988.
(67) Mehrotra, R. C. *J. Indian Chem. Soc.* **1953**, *30*, 585−591.

(*R*)-2-Methoxy-2-(trifluoromethyl)phenylacetate of (*R*)-Methyl Lactate (8).[68] A dry NMR tube under N_2 was loaded with pyridine (0.3 mL) and $CDCl_3$ (0.3 mL). In the drybox, the tube was loaded with (*S*)-(+)-α-methoxy-α-(trifluoromethyl)phenylacetyl chloride (26.2 μL, 0.14 mmol) and (*R*)-lactic acid methyl ester (9.55 μL, 0.10 mmol). The tube was shaken vigorously and allowed to stand overnight at room temperature. Excess *N*,*N*-dimethyl-1,3-propanediamine (24 μL, 0.20 mmol) was added and the mixture allowed to stand for 5 min. The mixture was diluted with ether (15 mL) and washed with cold 1 N HCl (3 × 10 mL), saturated Na_2CO_3 (3 × 10 mL), and brine (3 × 10 mL). The organic phase was dried (Na_2SO_4), filtered, and concentrated in vacuo, yielding a yellow oil. Yield: 0.029 g. ^{1}H NMR ($CDCl_3$, 300 MHz): δ 7.60−7.63 (2H, m), 7.38−7.43 (3H, m), 5.23−5.31 (1H, q), 3.78 (3H, s), 3.65 (3H, br s), 1.51 (3H, d, J = 7.5).

(*R*)-2-Methoxy-2-(trifluoromethyl)phenylacetate of (*S*)-Methyl Lactate (9). The method described for the synthesis of **8** was used for the synthesis of **9**, from (*S*)-(+)-α-methoxy-α-(trifluoromethyl)phenylacetyl chloride and (*S*)-lactic acid methyl ester. Yield: 0.028 g. ^{1}H NMR ($CDCl_3$, 300 MHz): δ 7.55−7.60 (2H, m), 7.39−7.43 (3H, m), 5.26−5.34 (1H, q), 3.74 (3H, s), 3.57 (3H, br s), 1.58 (3H, d, J = 7.5).

General Procedure for Kinetics Studies. A series of 4 mL vials in the drybox were loaded with a small amount of lactide, catalyst from a stock solution in toluene ([lactide]/[Al] = 100), and dry toluene (lactide concentration in toluene was 0.2 M). The reaction vials were sealed tightly, removed from the drybox, and heated to 70 °C via an oil bath. After specified time intervals, each reaction was quenched via rapid cooling with liquid N_2. The solvent was removed in vacuo and the percent conversion determined by ^{1}H NMR. Each reaction was used as one data point.

(68) Yasuhara, F.; Yamaguchi, S. *Tetrahedron Lett.* **1980**, *21*, 2827−2830.

Acknowledgment. This work was generously supported by the NSF (Career Award CHE-9875261), the Arnold and Mabel Beckman Foundation (Young Investigator Award to G.W.C.), the U.S. Department of Education (fellowship to T.M.O.), and The Dow Chemical Co. We thank Dr. B. Maughon (Dow) for helpful discussions, E. Lobkovsky for crystallography, and J. Bergman for the synthesis of (*R*)-**5**. This work made use of the Cornell Center for Materials Research Shared Experimental Facilities, supported through the National Science Foundation Materials Research Science and Engineering Centers program (Grant DMR-0079992), and the Cornell Chemistry Department X-ray Facility (supported by the NSF; Grant CHE-9700441). G.W.C. gratefully acknowledges a Camille and Henry Dreyfus New Faculty Award, a Research Corp. Research Innovation Award, an Alfred P. Sloan Research Fellowship, a Camille Dreyfus Teacher-Scholar Award, a David and Lucile Packard Foundation Fellowship in Science and Engineering, a 3M Untenured Faculty Grant, and a Union Carbide Innovation Recognition Award.

Supporting Information Available: X-ray crystal structures and crystallographic data for (*R*)-**3** and (*R*)-**5**, plots of ln([M_o/M_t]) vs time (lactide/**4**) and ln k_{app} vs ln [Al] (*meso*-lactide/(*R*)-**4**), and ^{13}C NMR spectra of heterotactic and stereoblock PLA (PDF). This material is available free of charge via the Internet at http://pubs.acs.org.

JA012052+